

Transport properties in liquids from first principles: the case of liquid water and liquid Argon

Pier Luigi Silvestrelli

Dipartimento di Fisica e Astronomia “G. Galilei”,

Università di Padova, via Marzolo 8, I-35131 Padova, Italy

(Dated: February 15, 2023)

Abstract

Shear and bulk viscosity of liquid water and Argon are evaluated from first principles in the Density Functional Theory (DFT) framework, by performing Molecular Dynamics simulations in the NVE ensemble and using the Kubo-Greenwood equilibrium approach. Standard DFT functional is corrected in such a way to allow for a reasonable description of van der Waals (vdW) effects. For liquid Argon the thermal conductivity has been also calculated. Concerning liquid water, to our knowledge this is the first estimate of the bulk viscosity and of the shear-viscosity/bulk-viscosity ratio from first principles. By analyzing our results we can conclude that our first-principles simulations, performed at a nominal average temperature of 366 K to guarantee that the systems is liquid-like, actually describe the basic dynamical properties of liquid water at about 330 K. In comparison with liquid water, the normal, monatomic liquid Ar is characterized by a much smaller bulk-viscosity/shear-viscosity ratio (close to unity) and this feature is well reproduced by our first-principles approach which predicts a value of the ratio in better agreement with experimental reference data than that obtained using the empirical Lennard-Jones potential. The computed thermal conductivity of liquid Argon is also in good agreement with the experimental value.

I. INTRODUCTION

Transport properties are among the most important and useful features of condensed-matter systems, particularly for characterizing the dynamical behavior of liquids, since they play an important role in many technical and natural processes. Therefore their estimate represents one of the most relevant goal of Molecular Dynamics (MD) simulation techniques which become particularly useful in cases where experimental data are not available or difficult to obtain. Different theoretical approaches can be adopted with a varying degree of accuracy (see, for instance, refs. 1–35, and further references therein).

Basically, in MD simulation transport properties can be evaluated either through a genuine *nonequilibrium approach* by applying an explicit external perturbation (such as a shear flow or a temperature gradient), which is clearly direct and intuitive but is affected by non-trivial technical issues (in particular the need to generate nonequilibrium steady states in typical systems characterized by finite-size supercells with periodic boundary conditions and to extrapolate to the limit of zero driving force). Alternatively, the transport coefficients can be more easily estimated from *equilibrium* MD simulations by using the Green-Kubo relations^{36–38} of statistical mechanics (dissipation-fluctuation theorem) which allow the calculation of transport coefficients by integration of suitable autocorrelation functions. This latter approach is simpler because standard equilibrium MD simulations can be easily carried out and estimated transport coefficients exhibit a weaker system-size dependence.²⁶ An equivalent¹⁷ equilibrium method exploits the Einstein–Helfand expressions² to get transport coefficients directly from the particle displacements and velocities;¹⁸ for instance, the shear viscosity can be computed in terms of the mean-square x displacement of the center of y momentum, while the thermal conductivity is proportional to the mean square x displacement of the center of energy.

The shear viscosity describes the resistance of a fluid to shear forces and is a measure of the shear stress induced by an applied velocity gradient,¹ while the bulk viscosity refers to the resistance to dilatation of an infinitesimal volume element at constant shape and measures the resistance of a fluid to compression. It is closely connected with absorption and dispersion of ultrasonic waves in a fluid, so it can provide valuable information about intermolecular forces. Moreover, the role of the bulk viscosity is acquiring more and more importance, for instance in the area of surface and interface-related phenomena and for

the interpretation of acoustic sensor data.³⁹ In spite of its relevance, bulk viscosity has received less experimental and theoretical attention, partly due to the greater difficulties in obtaining accurate measurements and estimates. In principle it should be evaluated in the microcanonical (NVE) ensemble where there is no need to evaluate an additional term which would be required if, for instance, the canonical NVT ensemble were used.^{13,39} Moreover, bulk viscosity is subject to much larger statistical error caused by the fact that it must be calculated by the regression of fluctuations about a nonzero mean.³ While the shear viscosity is associated with changes in water Hydrogen-bond network connectivity and is mostly related to translational molecular motion, the bulk viscosity is associated with local density fluctuations and reflects the relaxation of both rotational and vibrational modes.^{40,41} The thermal conductivity describes instead the capability of a substance to allow molecular transport of energy driven by temperature gradients.

In general dynamical properties such as the transport coefficients are much more dependent on the simulation size and timescale than structural properties.²³ One must also point out that shear and bulk viscosities, and thermal conductivity are even more difficult to be evaluated accurately than, for instance, the diffusion coefficient (a single-particle property) since they are *collective* transport properties involving all the particles.¹⁴ In fact, for estimating the diffusion coefficient one can perform a statistical average over the particles in addition to the average over time because every particle diffuses individually but any stress or energy fluctuation is an event involving the system as a whole. As a consequence, in order to obtain the same statistical accuracy, collective properties need much longer runs than single particle properties by a factor proportional to the size of the system.¹²

We here estimate from first principles simulations, in the framework of the Density Functional Theory (DFT), the shear and bulk viscosity of liquid water and Argon. For liquid Argon the thermal conductivity is also calculated. By analyzing our results we can conclude that our first-principles simulations, performed at a nominal average temperature of 366 K to guarantee that the systems is liquid-like, actually describe the basic dynamical properties of liquid water at about 330 K. Our approach is also able to reproduce well the bulk-viscosity/shear-viscosity ratio of liquid Ar which is much smaller than that of liquid water.

II. METHOD

We have performed first principles MD simulations of liquid water using the CPMD package,⁴² at constant volume, considering the experimental density of water at room temperature. The computations were performed at the Γ -point only of the Brillouin zone, using norm-conserving pseudopotentials⁴³ and a basis set of plane waves to expand the wavefunctions with an energy cutoff of 250 Ry; we have explicitly tested that this energy cutoff, much higher than that used in standard DFT simulations of liquid water, is required to have a good convergence also for the stress tensor components.

We have adopted the gradient-corrected BLYP⁴⁴ density functional augmented by van der Waals (vdW) corrections, hereafter referred to as DFT-D2(BLYP).⁴⁵ This choice is motivated both by the fact that BLYP has been shown⁴⁶⁻⁵⁰ to give an acceptable description of Hydrogen bonding in water, and because it represents a good reference DFT functional to add vdW corrections.⁵¹⁻⁵⁴ A good description of Hydrogen bonding is essential here since, in liquid water, the shear viscosity mostly originates from covalent interactions in the Hydrogen-bond dynamics of water molecules.¹⁹ Moreover, vdW corrections to BLYP are important because it was shown that BLYP significantly underestimates (by 25%) the equilibrium density of liquid water; the experimental density can be recovered by adding the vdW corrections proposed by Grimme,⁴⁵ which have the further effect of making the oxygen-oxygen radial distribution function in better agreement with experiment.^{55,56} Our system consists of 64 water molecules contained in a supercell with simple-cubic symmetry and periodic boundary conditions. Hydrogen nuclei have been treated as classical particles with the mass of the deuterium isotope which allows us to use larger time steps. The effective mass determining the time scale of the fictitious dynamics of the electrons was 700 a.u. and the equations of motion were integrated with a time step of 3 a.u. (=0.073 fs).

Our simulation consisted of an initial equilibration phase, lasting about 0.15 ps, in which the ionic temperature was simply controlled by velocity rescaling, followed by a much longer (about 22 ps) canonical (NVT) MD simulation (using suitable thermostats for a Nosé-Hoover dynamics), followed by a final 22 ps microcanonical (NVE) production MD run. A common drawback of most standard DFT functionals applied to liquid water at room temperature is their tendency to "freeze" the system which therefore exhibits an ice-like behavior. By applying vdW corrections the problem is reduced but it still present. In particular, since

the melting temperature of water estimated by DFT-D2(BLYP) is 360 K⁵⁷ (while it is 411 K with BLYP), following a common strategy,^{29,32,33,58} we performed NVT simulations with an average ionic temperature of 380 K to be sure that the system is indeed liquid-like. This use of artificially increased temperature also serves to mimic Nuclear Quantum Effects in simulations of liquid water.²³ The average ionic temperature of the subsequent NVE MD simulation was 366 K. Several data (atomic coordinates, velocities, stress-tensor components,...) relevant for characterizing structural and dynamical properties of the system were recorded every 20 steps in the production stage.

As far as liquid Ar is concerned, before starting MD simulations, we have performed extensive preliminary calculations to choose optimal parameters and a suitable DFT functional. Clearly in this case even an empirical Lennard-Jones potential reference could probably give reasonable results but here we are interested in studying transport properties using DFT functionals in a first-principle framework, which has the advantage of explicitly accounting for the electronic structure of matter. Application to the face-centered cubic (fcc) Ar crystal (considering a fcc supercell with 32 Ar atoms) and comparison with experimental reference values for the equilibrium Ar-Ar distance and the cohesive energy, suggests that, among many tested, vdW-corrected DFT functionals, DFT-D2(PBE)^{45,59} is the most adequate to describe extended systems made by Ar atoms, hence we mainly use it for the MD simulations of liquid Ar. In this case we have checked that a suitable energy cutoff to get a good convergence for the stress tensor components is 110 Ry.

The liquid Ar sample was prepared starting from an initial (unfavorable) simple cubic lattice configuration with 64 Ar atoms and considering the experimental Ar density (1.4 g/cm³) at melting point (84 K). Then the systems was heated by gradually increasing the ionic temperature (by velocity rescaling) to 500 K (in a time of 1.3 ps) to be sure that the system was truly melted; then the temperature was gradually decreased (in 1.0 ps) to 150 K, which is a temperature sufficiently higher than the experimental melting point that it can be assumed that the system is indeed in a liquid phase; this has been explicitly checked looking at the translational order parameter.¹

Then a 60 ps canonical (NVT) MD simulation (with a ionic temperature of 150 K) was performed, followed by a 60 ps microcanonical (NVE) MD production runs with an average ionic temperature of 129 K. In this case the electronic effective mass was 700 a.u. and the equations of motion were integrated with a time step of 5 a.u. (=0.121 fs). Data (atomic

coordinates, velocities, stress-tensor components,...) relevant for structural and dynamical properties of the system were recorded every 10 steps in the production stage.

As mentioned above, different approaches exist for the calculation of shear, η_S , and bulk, η_B , viscosity from MD simulations.^{1,8-11,13} The most used technique is based on the evaluation of the autocorrelation functions of stress-tensor components; in particular,¹

$$\eta_S = \frac{V}{k_B T} \int_0^\infty dt \langle P_{\alpha\beta}(0) P_{\alpha\beta}(t) \rangle, \quad (1)$$

$$\eta_B = \frac{V}{9k_B T} \int_0^\infty dt \langle \delta P_{\alpha\alpha}(0) \delta P_{\beta\beta}(t) \rangle = \frac{V}{k_B T} \int_0^\infty dt \langle \delta P(0) \delta P(t) \rangle, \quad (2)$$

where, in practice the upper limit of integration (∞) is replaced by a reasonably-long simulation time, t_{max} , $\langle \dots \rangle$ denotes average over different time origins, V is the system volume, T the ionic temperature, k_B the Boltzmann constant, $P_{\alpha\beta}$ quantities denote the components of the stress tensor, the instantaneous pressure is given by $P(t) = 1/3 \sum_\alpha P_{\alpha\alpha}$ (that is the average of the diagonal elements of the stress tensor), and the fluctuations are defined as:

$$\delta P_{\alpha\alpha}(t) = P_{\alpha\alpha}(t) - \langle P_{\alpha\alpha} \rangle = P_{\alpha\alpha}(t) - P, \quad \delta P(t) = P(t) - \langle P \rangle = P(t) - P, \quad (3)$$

where P is the system pressure obtained as the ensemble average of $P(t)$. In isotropic fluids (with rotational invariance) there are only 5 independent (and equivalent) components of the traceless stress tensor: P_{xy} , P_{yz} , P_{zx} , $(P_{xx} - P_{yy})/2$, and $(P_{yy} - P_{zz})/2$, so that it is convenient to compute the shear viscosity η_S by averaging over these 5 components to get better statistics.

Instead, the bulk viscosity η_B has only one component, moreover the diagonal stresses must be evaluated carefully since a non-vanishing equilibrium average must be subtracted. In order to get more accurate evaluations of transport properties and also reliable estimates of the associated statistical errors, we adopt the block-average technique,⁶⁰ which consists of dividing the whole simulation into a sequence of several shorter intervals (“blocks”), each with an equal number of samples; then block averages are calculated which allow to estimate means and variances.¹⁵ In the case of the bulk-viscosity calculation, to reduce the error, it is convenient to take for the system pressure the average value of the pressures over all blocks.¹³ Clearly the choice of the block size must be made with care; in fact,

samples become uncorrelated as the block size increases so for small block sizes, the error is underestimated while for large block sizes the error estimate is inaccurate due to insufficient sampling (see detailed discussion below).

Typically transport coefficients are estimated from classical MD simulations based on empirical interatomic potentials. The practical feasibility of calculating transport coefficients in liquids using instead first principles MD simulations, was demonstrated by D. Alfé and M. J. Gillan,¹² who used the Green-Kubo relations¹² to compute the shear viscosity of liquid iron and aluminum, with a statistical error of about 5%. However, the simulations of D. Alfé and M. J. Gillan¹² were performed in the NVT ensemble, while our simulations have been carried out using the NVE ensemble, since the NVE simulations also allow the evaluation of the bulk viscosity without any correction term (see above). Subsequently, the problem of atomic heat transport and the development of a microscopic theory for the calculation of the thermal conductivity within the Green-Kubo formalism, by a first-principles DFT approach, has been successfully addressed by Marcolongo *et al.*^{29–31} Efficient, first-principles evaluations of thermal conductivity and shear viscosity have been also recently proposed.^{32–35}

A simpler alternative method exists (valid for temperatures that are not too low⁶¹) to obtain an approximate estimate of the shear viscosity, by exploiting its connection with the self-diffusion coefficient D via the Stokes-Einstein relation:^{4,12}

$$\eta_S = \frac{k_B T}{2\pi a D}, \quad (4)$$

where a is an effective atomic diameter. Such relation is exact for the Brownian motion of a macroscopic particle of diameter a in a liquid of shear viscosity η_S , but it is only approximate when applied to atoms; however if a is chosen to be the radius r_1 of the first peak in the radial distribution function, the relation usually predicts η_S to within 40%.¹² Here we take for r_1 the position of the first peak in the O-O and Ar-Ar radial distribution function for liquid water and liquid Ar, respectively, while the diffusion coefficient D can be computed¹ from the mean square displacement of the oxygen atoms (for liquid water) or Ar atoms (for liquid Ar). The validity of the Stokes-Einstein relation has been recently discussed in detail by Herrero *et al.*⁶¹ who also explored the connection between structural properties and transport coefficients.

For liquid Argon the thermal conductivity has been also calculated, using the formula:¹

$$\lambda_T = \frac{V}{k_B T^2} \int_0^\infty dt \langle j_\alpha^E(0) j_\alpha^E(t) \rangle, \quad (5)$$

where j_α^E is the α component of the energy current defined as the time derivative of

$$\delta E_\alpha = \frac{1}{V} \sum_i r_{i\alpha} (E_i - \langle E_i \rangle), \quad (6)$$

and E_i is the energy of the i -th Ar atom (located at coordinates r_{ix}, r_{iy}, r_{iz}), which can be evaluated as

$$E_i = p_i^2/2m_i + 1/2 \sum_{j \neq i} v(r_{ij}), \quad (7)$$

by assuming a *pairwise* interatomic potential. In order to obtain a pair potential for evaluating the thermal conductivity of liquid Ar using configurational data from our first-principles DFT simulations, we have adopted a strategy similar to that proposed in ref. 26: we assume for the pair potential a Lennard-Jones analytical form:

$$v(r) = a(b^2/r^{12} - b/r^6), \quad (8)$$

where a and b are parameters optimized by fitting the potential-energy curve of the Ar dimer (at different interatomic distances) obtained by using our DFT approach. Admittedly, such an approach is rather approximated and could represent only a rough estimate of the thermal conductivity. A more fundamental and accurate method has been recently proposed.²⁹⁻³¹

III. RESULTS AND DISCUSSION

In Fig. 1 and 2 we plot the behavior of the temperature and pressure as a function of time in the NVE simulation for liquid water and Ar, respectively. As can be seen, these quantities turn out to be stable and exhibit only moderate oscillations around the average values, which are, for liquid water, 0.132 GPa and 366 K for the pressure and the temperature, respectively, while for liquid Ar the values are 0.173 GPa and 129 K.

In Fig. 3 and 4 we instead plot the auto-correlation functions (ACFs), corresponding to the integrands (considering the average over the components for the shear viscosity) of eqs. (1) and (2). Differently from what observed in monatomic systems (such as liquid Ar) or

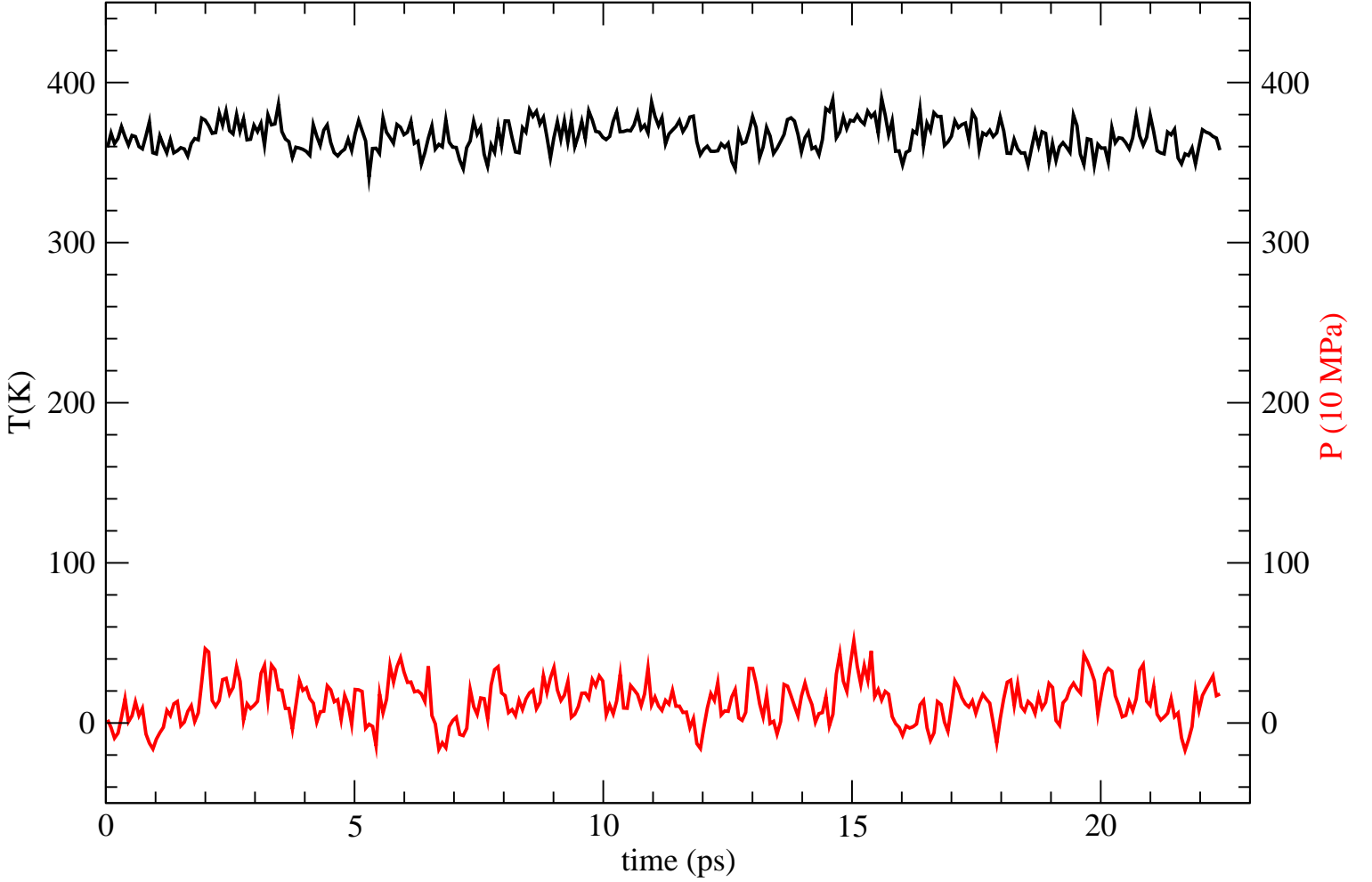


FIG. 1: Temperature and pressure of liquid water plotted as a function of the simulation time.

in classical MD simulations where waters are modeled by rigid molecules, in first-principles simulations of liquid water, high-frequency intermolecular vibrations lead to corresponding high-frequency oscillations in the pressure and in related ACFs. In order to better appreciate the global decay behavior of ACFs, in the case of liquid water, high-frequency components have been cut by Fourier-transforming the ACFs. A quantitative estimate of the ACFs relaxation times can be obtained assuming a global exponential decay ($\simeq e^{-t/\tau}$) of the

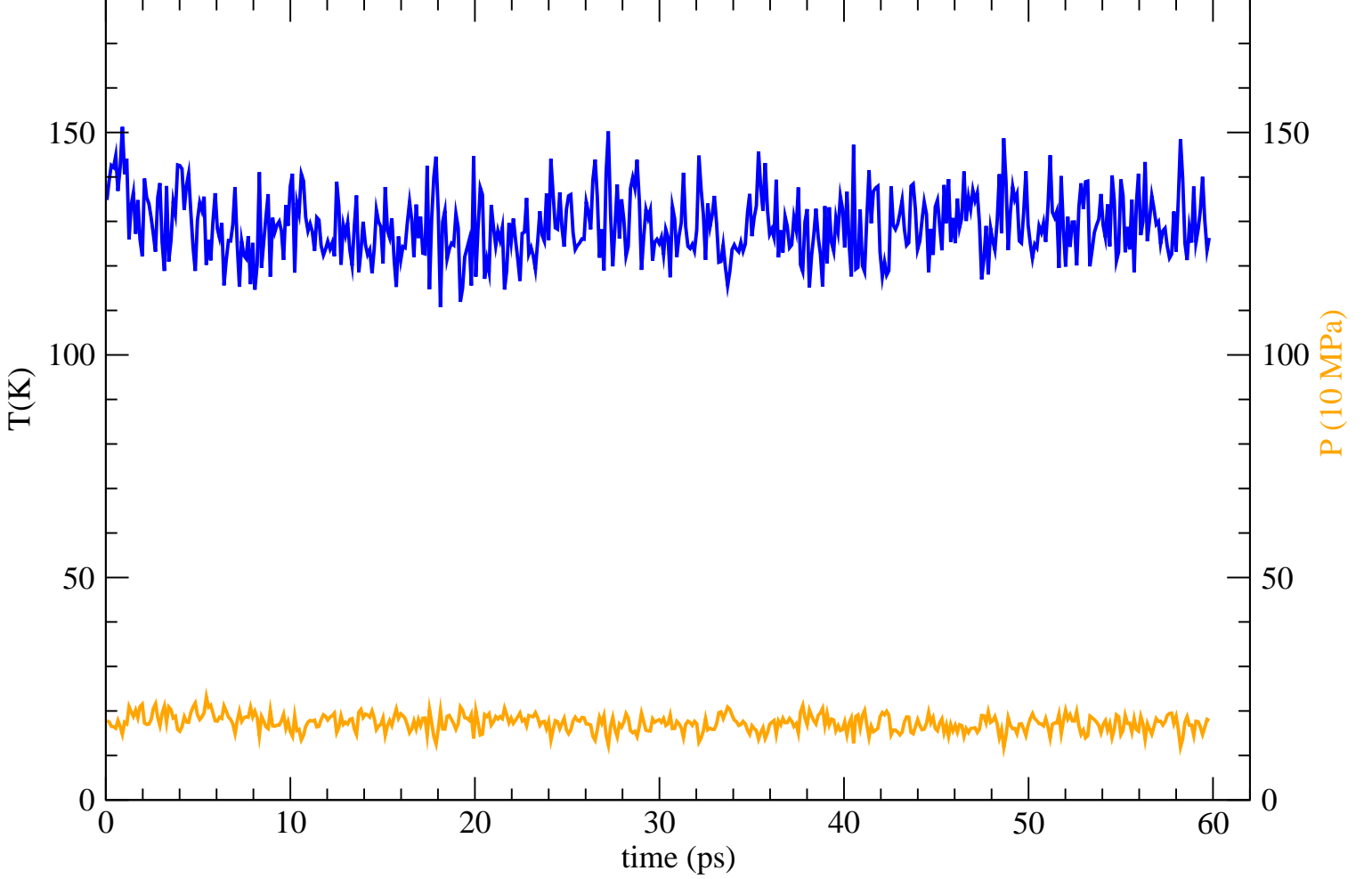


FIG. 2: Temperature and pressure of liquid Ar plotted as a function of the simulation time.

integrands and computing:

$$\tau_S = \int_0^\infty dt \frac{\langle P_{\alpha\beta}(0)P_{\alpha\beta}(t) \rangle}{\langle P_{\alpha\beta}(0)P_{\alpha\beta}(0) \rangle}, \quad (9)$$

and

$$\tau_B = \int_0^\infty dt \frac{\langle \delta P_{\alpha\alpha}(0)\delta P_{\beta\beta}(t) \rangle}{\langle \delta P_{\alpha\alpha}(0)\delta P_{\beta\beta}(0) \rangle} \quad (10)$$

For liquid water we find $\tau_S \simeq 6$ fs and $\tau_B \simeq 4$ fs, while for liquid Ar $\tau_S \simeq 340$ fs and $\tau_B \simeq 410$ fs.

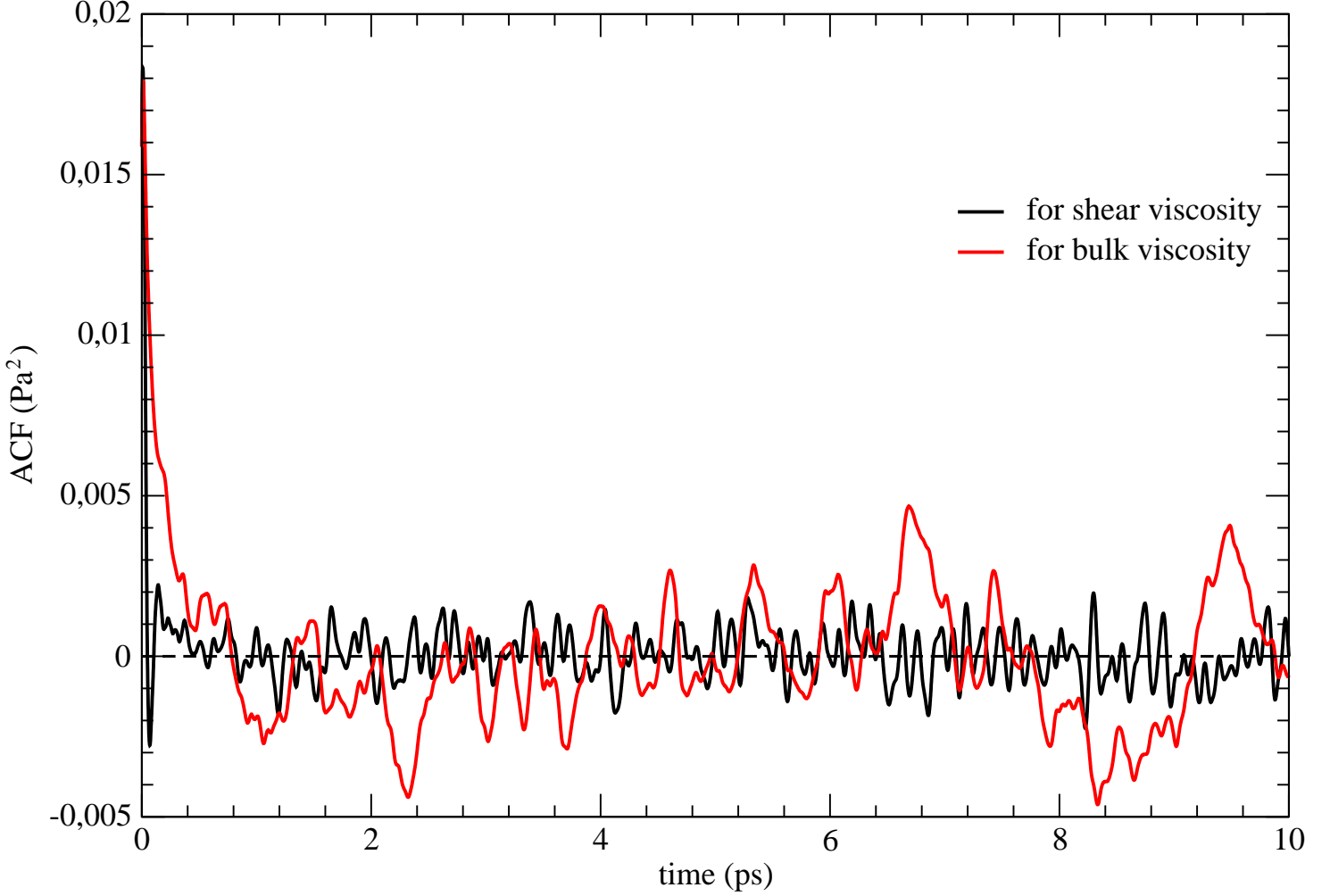


FIG. 3: Auto-correlation functions (ACFs) used for the evaluation of the shear and bulk viscosities of liquid water (see text) plotted as a function of the simulation time.

The shear and bulk viscosity, computed using eqs. (1) and (2), are plotted as a function of the upper limit of the integrals in Fig. 5 and 6, while the thermal conductivity of liquid Ar is reported in Fig. 7. From these curves an approximate estimate of the shear and bulk viscosity can be obtained considering the values of the quantities corresponding to the position of the first pronounced maximum-plateau; in fact this indicates that the running integral starts becoming nearly independent of time implying that the corresponding ACF

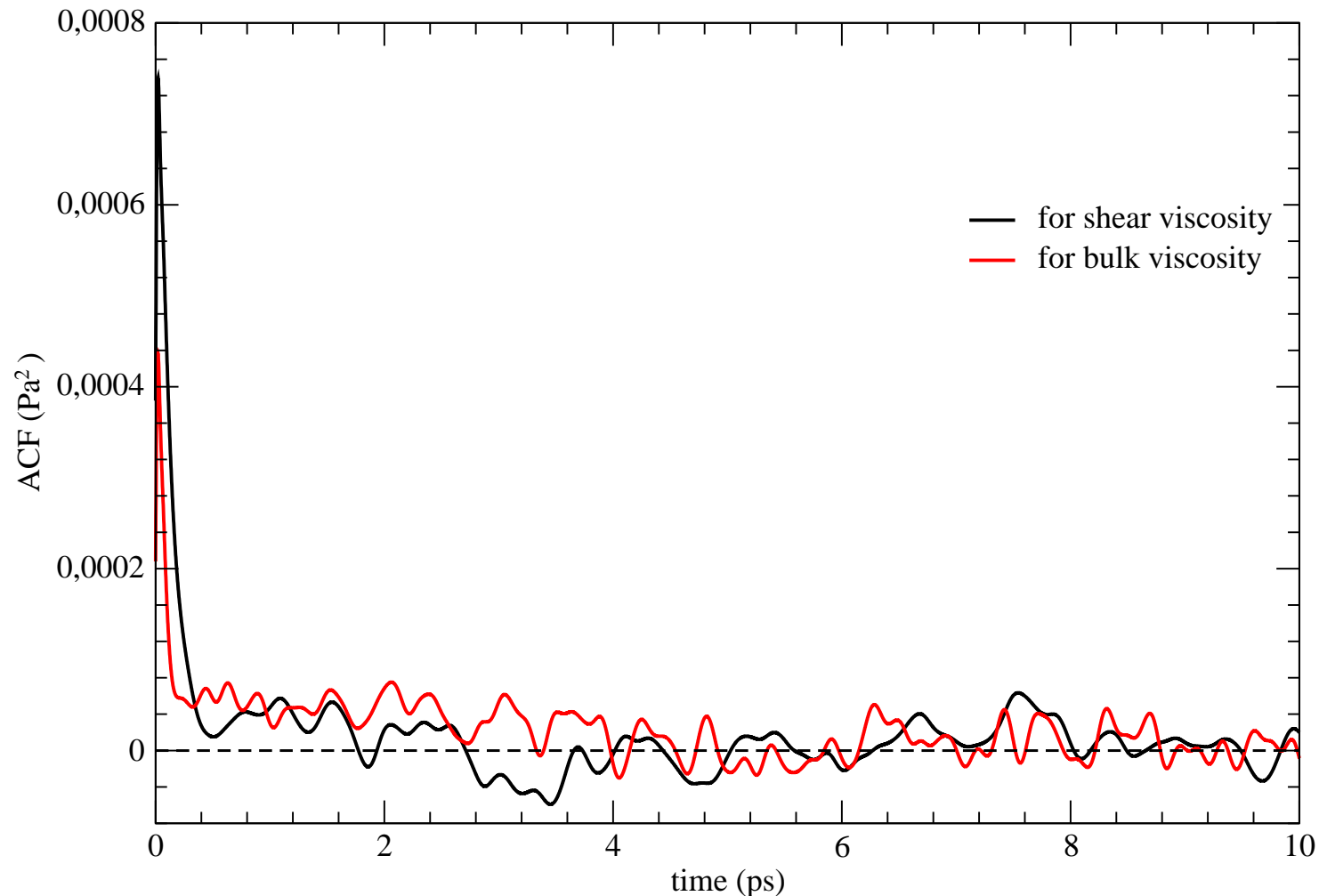


FIG. 4: Auto-correlation functions (ACFs) used for the evaluation of the shear and bulk viscosities of liquid Ar (see text) plotted as a function of the simulation time.

has decayed to zero and is fluctuating along the horizontal time axis. Clearly, considering longer times only introduces additional noise to the signal and the beginning of a plateau represents the desired value of the viscosity with the smallest uncertainty. As can be seen, the maximum-plateau is reached at about $t = 0.8$ ps for both the shear and bulk viscosity of liquid water, while the corresponding values for liquid Ar are 3.0, 5.0 ps, and 0.5 ps for the shear viscosity, the bulk viscosity, and the thermal conductivity, respectively. As expected,

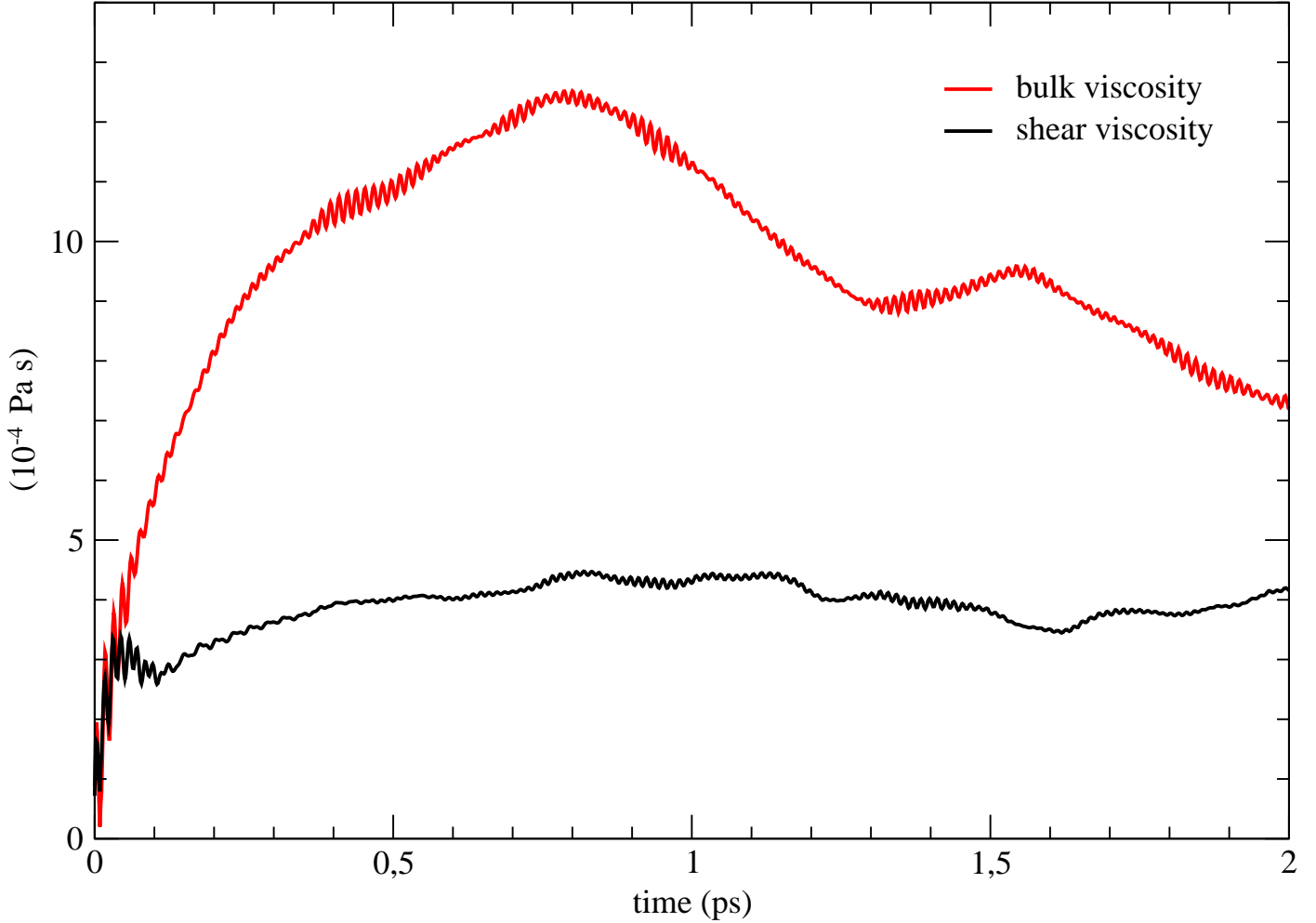


FIG. 5: Shear and bulk viscosity of liquid water plotted as a function of the upper limit of the integrals of the ACFs.

these times are much larger than the corresponding relaxation times τ_S and τ_B estimated above.

As already discussed, a more accurate evaluation, with also a reliable estimate of the associated statistical error, can be obtained by adopting a block-average technique. In this case a proper choice of the block size is crucial: with many, small-size blocks, the statistical error is small but the blocks are probably correlated and the viscosity is typically

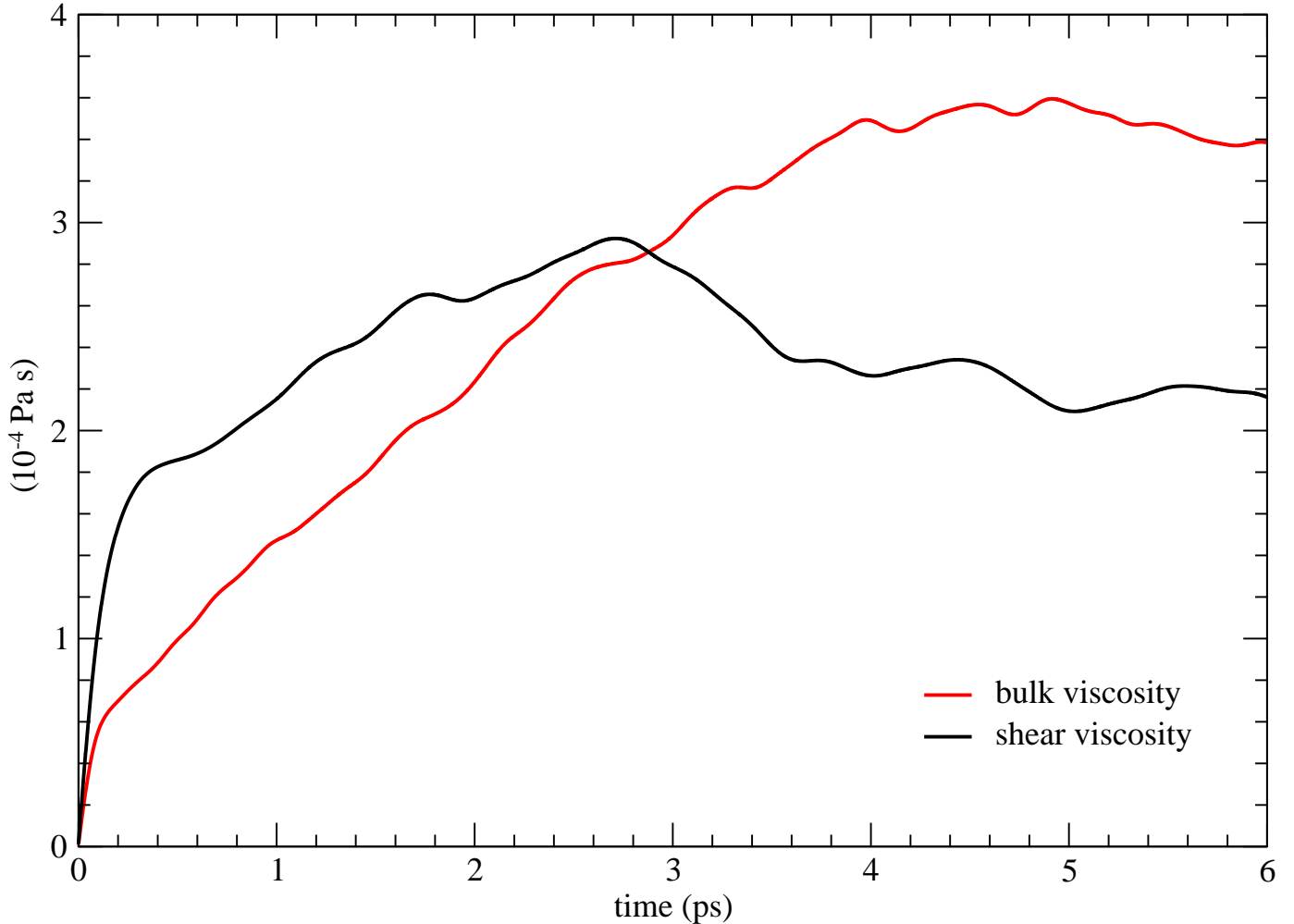


FIG. 6: Shear and bulk viscosity of liquid Ar plotted as a function of the upper limit of the integrals of the ACFs.

underestimated (not yet converged); on the contrary, with just a few, large-size blocks, these are probably uncorrelated and the viscosity is converged but the statistical error is large.

In Figs. 8, 9, 10, and 11 we plot the values of the shear and bulk viscosity of liquid water and Ar evaluated by using different numbers of blocks (keeping constant the total number of configurations) with the relative statistical errors. The dashed horizontal lines indicate the corresponding values inferred by considering the maximas-plateaus of the curves

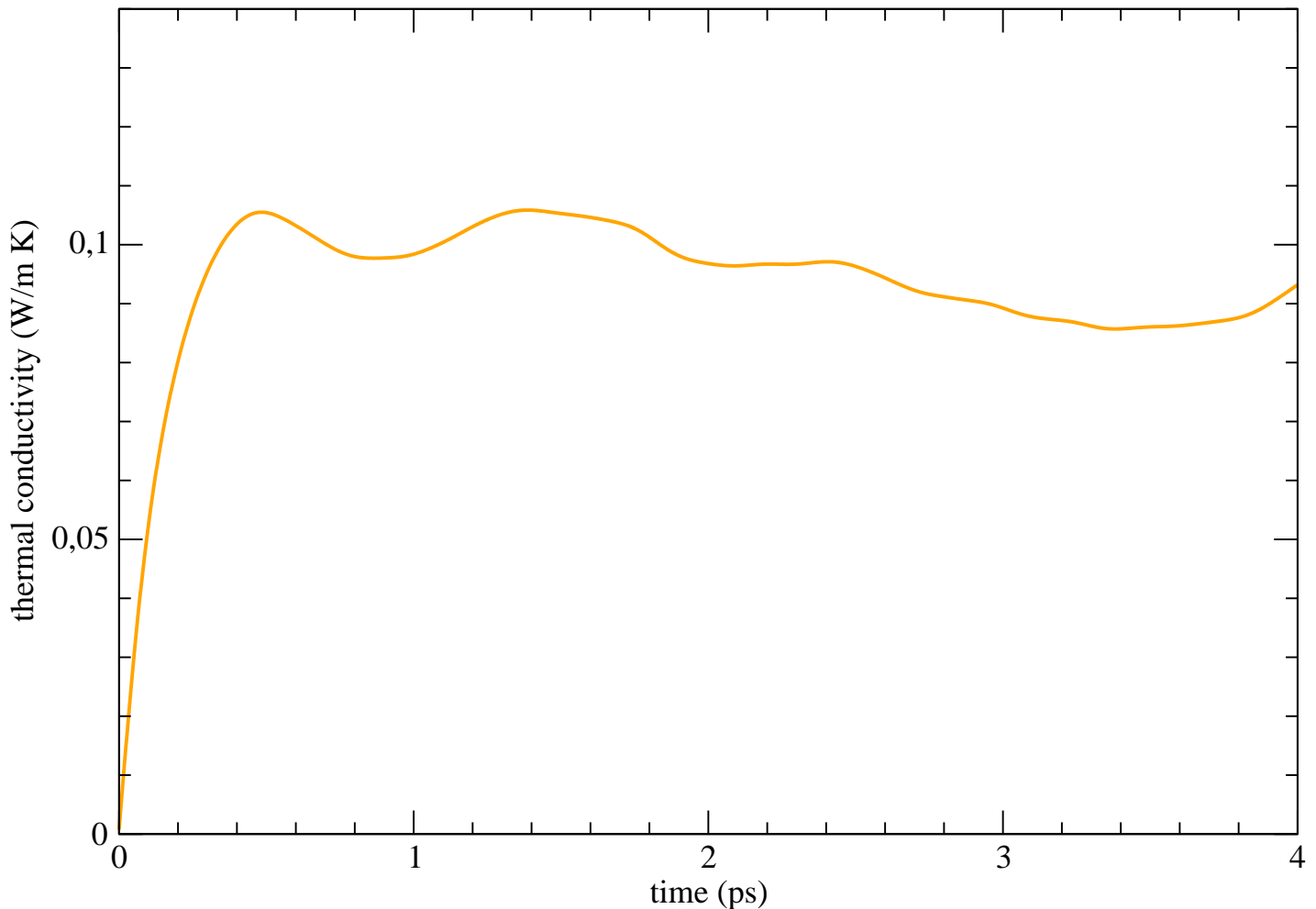


FIG. 7: Thermal conductivity of liquid Ar plotted as a function of the upper limit of the integral of the ACF.

in Figs. 5 and 6. As can be seen, in the case of liquid water, the maxima of the shear and bulk viscosities are obtained considering 16 blocks, each equivalent to a simulation time of about 1.4 ps. Interestingly, taking statistical uncertainties into account, these maxima are compatible with the rough estimates obtained before and, for the shear viscosity, also with the values obtained using the Stokes-Einstein formula (Eq. (4)). As already described above, in the Stokes-Einstein estimate the shear viscosity is obtained in terms of the diffusion

coefficient D and the radius of the first peak in the radial distribution function (see Eq. (4), for liquid water we have considered the first peak in the oxygen-oxygen radial distribution function, see below). Actually our reported Stokes-Einstein estimated values are corrected by finite-size effects: in fact D can be extrapolated to infinite size of the simulation box (see, for instance, ref. 61) by just considering the shear-viscosity value:

$$D_\infty = D + 2.837 \frac{k_B T}{6\pi\eta_S L}, \quad (11)$$

where L is the size of the cubic simulation box. Therefore, by simultaneously taking into account Eqs. (4) and (11), one can get a “self-consistent”, finite-size corrected Stokes-Einstein estimate for η_S :

$$\eta_S^* = \frac{k_B T}{2\pi a D} - 2.837 \frac{k_B T}{6\pi L D}. \quad (12)$$

Quantitative data are collected in Table I where they are also compared with some theoretical and experimental reference values.

As far as the shear viscosity is concerned, for liquid water our estimated value, obtained from the NVE simulation at an average temperature of 366 K, agrees with the experimental reference data at a lower temperature of about 330 K. This is in line with the performances of other DFT functionals; for instance (see Table I), in recent simulations⁶¹ of liquid water based on the SCAN functional,⁶⁸ the shear viscosity estimate is close to that obtained from a force-field approach (that, for this quantity, well reproduces the experimental behavior) only between 330 and 360 K, while it is severely overestimated at 300 K. A similar behavior has been found for the SCAN functional by Malosso *et al.*,³³ who computed the shear viscosity of liquid water from first-principles and deep-neural-network simulations. With the OPTB88-vdW functional⁶⁹ reasonable agreement with experimental data at room temperature is only found⁶¹ at 360 K, while with the PBE functional⁵⁹ this is only true at 454 K.³³

For liquid Ar the behavior is qualitatively similar (see Figs. 10, 11, and 12 for the shear viscosity, the bulk viscosity, and the thermal conductivity, respectively). In this case both the maxima of the shear and bulk viscosities are obtained considering 5 blocks, each equivalent to a simulation time of about 12.0 ps. Even in this case, taking statistical uncertainties into account, these maxima are compatible with the plateau positions and, for the shear viscosity, also with the estimate from the Stokes-Einstein formula. The maximum of the

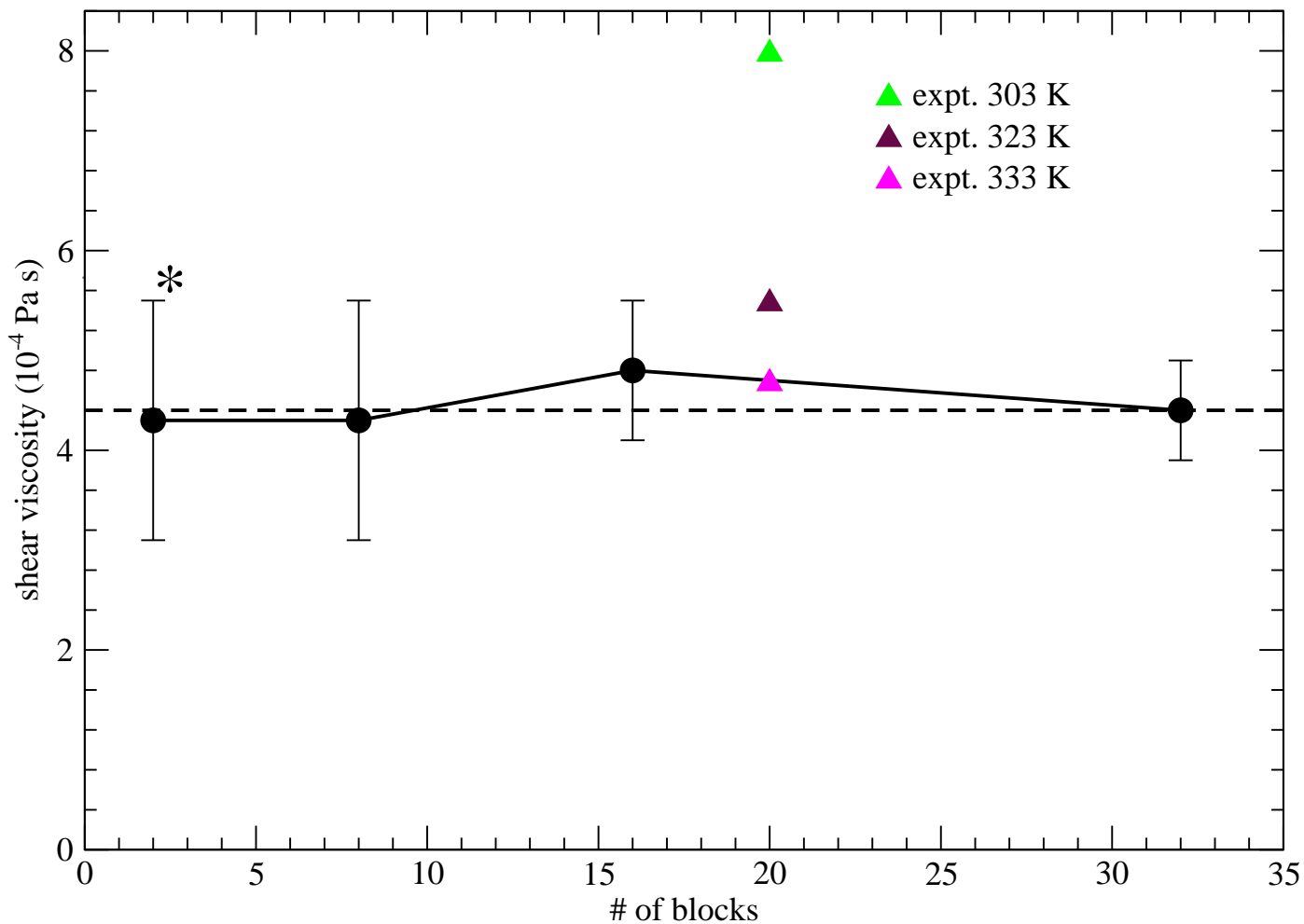


FIG. 8: Shear viscosity of liquid water evaluated by using different numbers of blocks (the smaller is the block number the larger is the number of configurations of each block) with the relative statistical errors. The dashed horizontal line indicates the position of the first-pronounced maximum-plateau of the corresponding curve of Fig. 5. The asterisk denotes the value obtained by the Stokes-Einstein formula (Eq.12), while the triangles indicate experimental estimates at different temperatures.

TABLE I: Shear and bulk viscosity of liquid water and Ar, in 10^{-4} Pa s, compared with theoretical and experimental reference data. Statistical errors are in parenthesis. η_S^* indicates the shear viscosity estimate obtained by the Stokes-Einstein relation (see text).

system	η_S	η_S^*	η_B	η_B/η_S	$3/4\eta_B/\eta_S + 1$
water (366 K)	4.8(0.7)	5.7	11.3(2.9)	2.4(0.8)	2.8(0.6)
water DFT SCAN ^a (300K)	23	—	—	—	—
water DFT SCAN ^a (330K)	6	—	—	—	—
water DFT SCAN ^a (360K)	5	—	—	—	—
water DFT OPTB88-vdW ^a (300K)	30	—	—	—	—
water DFT OPTB88-vdW ^a (330K)	15	—	—	—	—
water DFT OPTB88-vdW ^a (360K)	8	—	—	—	—
water force field ^a (300K)	8	—	—	—	—
water force field ^a (330K)	5	—	—	—	—
water force field ^a (360K)	3.5	—	—	—	—
water force field ^b (303K)	6.5(0.4)	—	15.5(1.6)	2.4(0.3)	2.8(0.2)
water expt. ^c (298 K)	8.90	—	—	—	—
water expt. ^{b,d,e} (303 K)	7.97	—	21.5	2.7	3.0
water expt. ^f (323 K)	5.47	—	14.8	2.7	3.0
water expt. ^c (333 K)	4.67	—	—	—	—
Ar (129 K)	3.7(1.6)	2.0	4.0(2.2)	1.1(0.8)	1.8(0.6)
Ar expt. ^g (90 K)	2.33	—	1.82	0.8	1.6
Ar expt. ^h (90 K)	2.57	—	—	—	—

^aref.61.

^bref.13.

^cref.64.

^dref.62.

^eref.63.

^fref.65.

^gref.66.

^href.67.

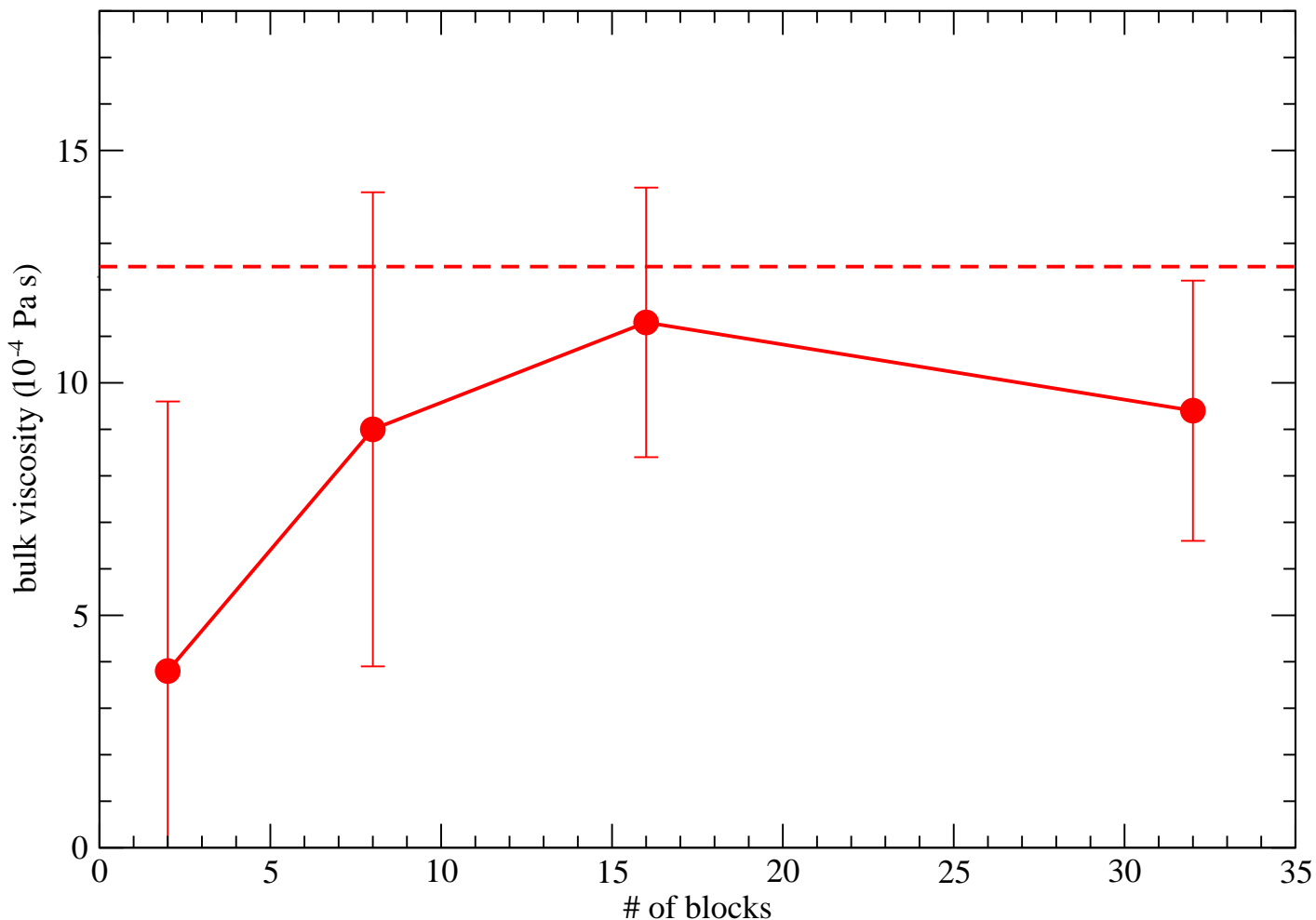


FIG. 9: Bulk viscosity of liquid water evaluated by using different numbers of blocks (the smaller is the block number the larger is the number of configurations of each block) with the relative statistical errors. The dashed horizontal line indicates the position of the first-pronounced maximum-plateau of the corresponding curve of Fig. 5.

thermal conductivity is instead reached with 25 blocks, each equivalent to a simulation time of about 2.4 ps, and its value (0.11 ± 0.02 W/m K) is again compatible with that estimated considering the maximum-plateau position and in good agreement with the literature reference value (0.12 W/m K) at 90 K⁷⁰ and that obtained by classical MD simulations based

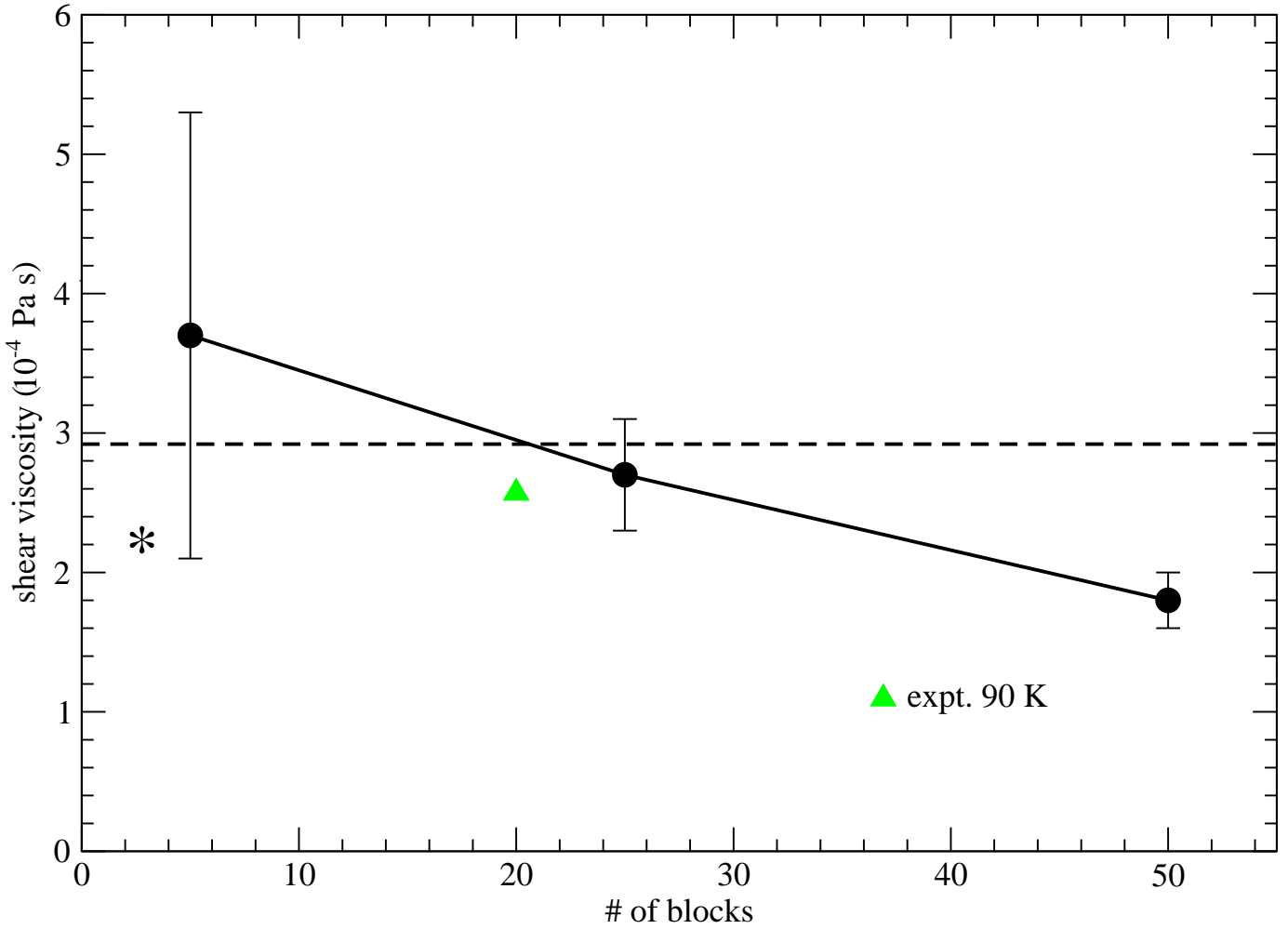


FIG. 10: Shear viscosity of liquid Ar evaluated by using different numbers of blocks (the smaller is the block number the larger is the number of configurations of each block) with the relative statistical errors. The dashed horizontal line indicates the position of the first-pronounced maximum-plateau of the corresponding curve of Fig. 6. The asterisk denotes the value obtained by the Stokes-Einstein formula (Eq.4), while the triangle indicates the experimental estimate at 90 K.

on the Lennard-Jones potential (0.119 W/m K).⁷¹ Accurate first-principles calculations of the thermal conductivity of liquid Ar have been carried out, at higher temperatures (250 and 400 K), by Marcolongo *et al.*²⁹, while the thermal conductivity of liquid water (adopting different DFT functionals) has been evaluated by Tisi *et al.*³² also using a deep neural network trained on DFT data.

An interesting physical quantity is represented by the ratio between bulk and shear viscosity, which can be related to the ratio of observed to classical absorption coefficients in

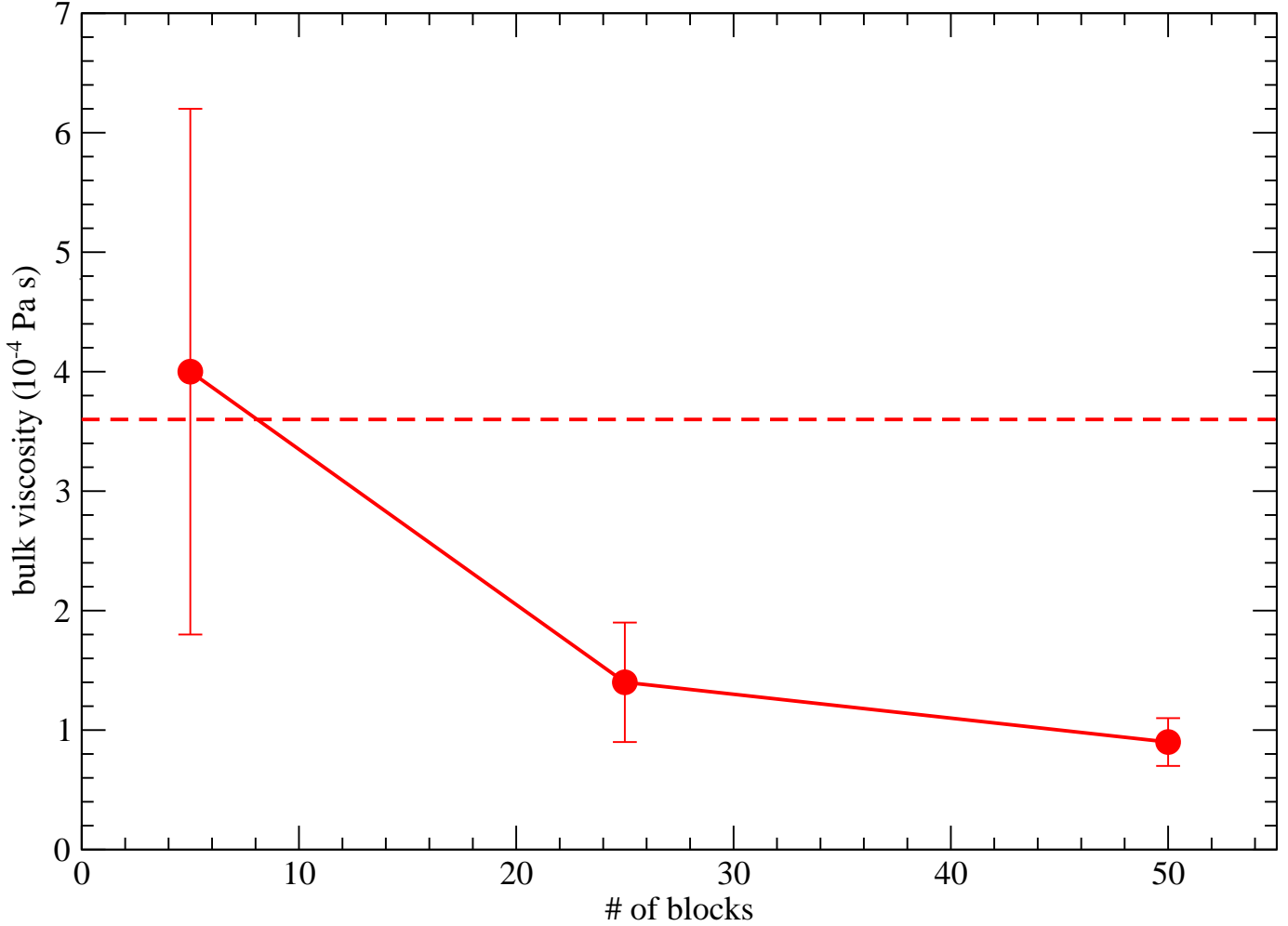


FIG. 11: Bulk viscosity of liquid Ar evaluated by using different numbers of blocks (the smaller is the block number the larger is the number of configurations of each block) with the relative statistical errors. The dashed horizontal line indicates the position of the first-pronounced maximum-plateau of the corresponding curve of Fig. 6.

ultrasonic absorption experiments.¹³ In fact, under the condition that the heat conductivity contribution to the ultrasonic absorption may be neglected,

$$\frac{\alpha}{\alpha_{class}} = 3/4 \frac{\eta_B}{\eta_S} + 1, \quad (13)$$

and water belongs to the group of the so-called "associated liquids", characterized by a

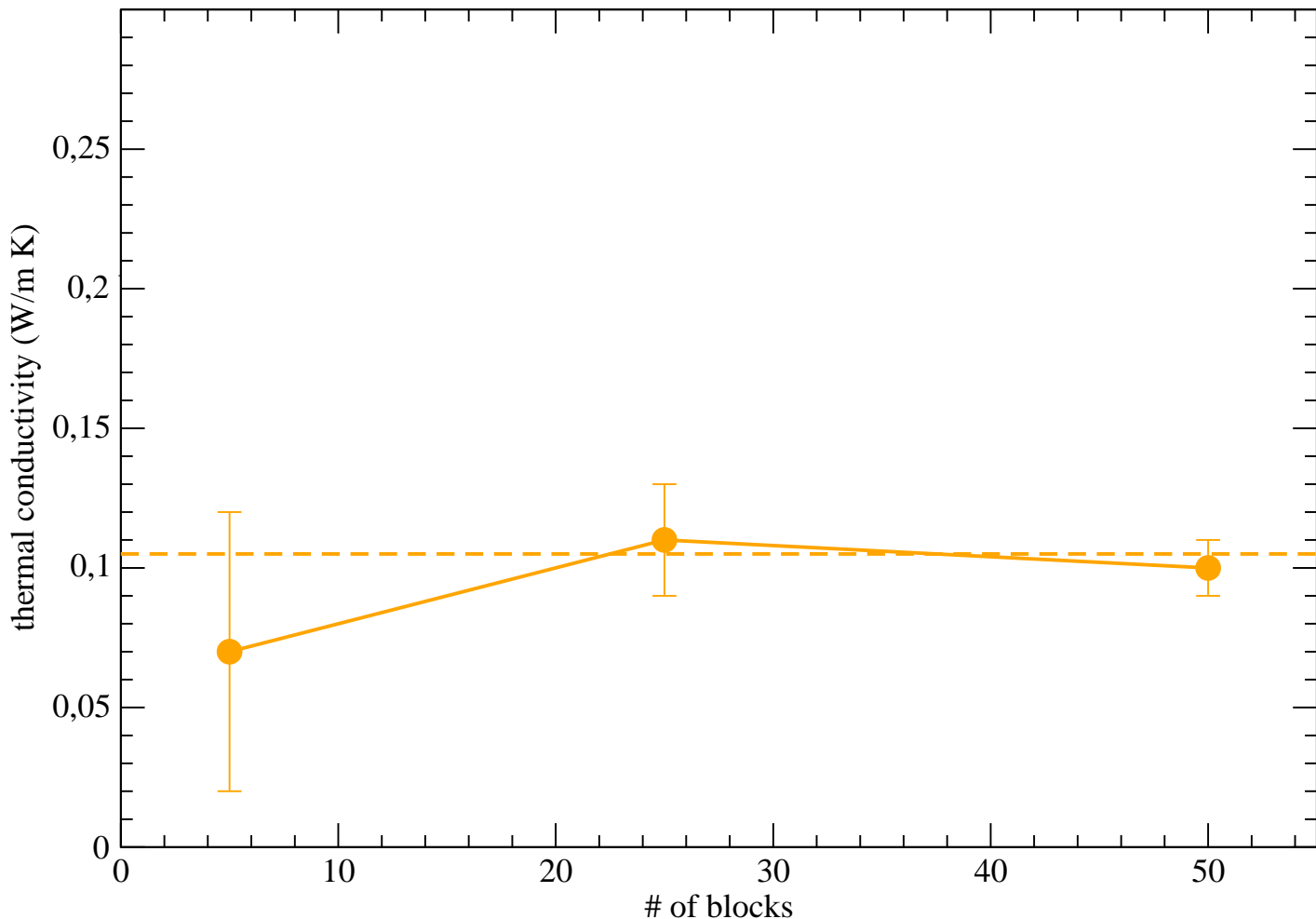


FIG. 12: Thermal conductivity of liquid Ar evaluated by using different numbers of blocks (the smaller is the block number the larger is the number of configurations of each block) with the relative statistical errors. The dashed horizontal line indicates the position of the maximum-plateau of the corresponding curve in Fig. 7.

ratio from 1 to 3, where structural relaxation is dominant.

Classical MD simulations based on the SPC/E semiempirical potential predict¹³ a $\frac{\eta_B}{\eta_S}$ ratio of 2.4, leading to a $\frac{\alpha}{\alpha_{class}}$ ratio of 2.79, in reasonable agreement with the experimental value of 3.0.⁶² Instead normal liquids, such as monatomic liquids (for instance liquid Ar) are characterized by a ratio no greater than 1.2. Although in general the ratio varies with

temperature and pressure, in liquid water it is found to remain constant within 20% in the temperature range 0-90 C (273-363 K).⁷² By taking statistical errors into account, our estimated value of the $\frac{\alpha}{\alpha_{class}}$ ratio (2.8 ± 0.6) is compatible with the available experimental data at ambient temperature (3.0). This is a remarkable result, considering that most of the reported classical MD simulations¹³ predict a bulk viscosity lower than the the experimental one, leading to an underestimated value of the $\frac{\alpha}{\alpha_{class}}$ ratio.

One should also point out that a proper comparison with experimental data requires a careful analysis taking into account the pronounced temperature dependence of shear and bulk viscosity. In fact, according to a common empirical model,^{65,73} the viscosity strongly decreases with increasing temperature following an exponential decay. By fitting experimental data⁶⁵ with an exponential function and taking statistical errors into account, our estimated values of the shear and bulk viscosity of liquid water are compatible with experimental data in the temperature range of 323-344 K. One should also consider that also the bulk-viscosity/shear-viscosity ratio for liquid water tends to decrease slightly with temperature,⁶⁵ suggesting an even better agreement between our estimated value and the experimental data.⁶⁵ We remind that our simulations have been carried out at temperatures higher than ambient temperature to guarantee that the systems is liquid-like. By considering that our estimate (after finite-size correction) for the diffusion coefficient, $D = 5.02 \times 10^{-5}$ cm²/s, corresponds to the experimental value measured at about 336 K,⁷⁴ we can conclude that, our DFT simulations based on the DFT-D2(BLYP) functional and performed at a nominal average temperature of 366 K, actually describe the basic dynamical properties of liquid water at about 330 K. One should also mention that bulk-viscosity measurements are indirect and affected by considerable errors.^{13,28,41,65,75,76} In summary, we can conclude that our adopted BLYP-D2 functional is able to describe reasonably well the density fluctuations of liquid water; the discrepancy with respect to experimental data at ambient conditions can be to a large extent explained in terms of the pronounced temperature dependence of both shear and bulk viscosity and the need to perform first-principles MD simulations at temperatures higher than ambient temperature, in line with the conclusions of other investigations.^{33,61}

As far as liquid Ar is concerned, our shear and bulk viscosities, computed by first-principles at a nominal average simulation temperature of 129 K, turn out to be somehow overestimated with respect to the reference experimental values at 90 K, although they are compatible with them if statistical errors are taken into account. Moreover our

TABLE II: Main features of the O-O pair correlation function, $g_{OO}(r)$, of liquid water and of the Ar-Ar pair correlation function, $g(r)$ of liquid Ar compared with experimental reference data, obtained from X-ray diffraction measurements at ambient conditions for liquid water and neutron-scattering measurements for liquid Ar. r_{max} and r_{min} indicate the position of the first maximum (the main peak) and the first minimum of $g_{OO}(r)$ and $g(r)$, respectively, and g_{max} and g_{min} the corresponding values of the $g_{OO}(r)$ and $g(r)$ functions.

system	$r_{max}(\text{\AA})$	g_{max}	$r_{min}(\text{\AA})$	g_{min}
water (366 K)	2.79	2.42	3.66	0.88
water expt. ^a (293 K)	2.80(1)	2.55(5)	3.41(4)	0.85(2)
Ar (129 K)	3.70	2.80	5.29	0.64
Ar expt. ^b (85 K)	3.68	3.05	5.18	0.56

^aref.77–79.

^bref.82.

bulk-viscosity/shear-viscosity ratio (close to unity) agrees well with the reference estimate, while interestingly this is not the case if a standard Lennard-Jones empirical potential is adopted using classical MD simulations that predict instead a very low value^{13,71} of the ratio (0.17-0.35 at high densities), thus showing that this popular potential cannot properly reproduce all the dynamical properties of liquid Ar and underlining once again the superiority of first-principles approaches.

We conclude our study by reporting some basic structural properties of our investigated systems. In particular, in Fig. 13, for liquid water we plot our computed O-O pair correlation function, $g_{OO}(r)$, compared with that obtained experimental from X-ray diffraction measurements at ambient conditions.^{77–79} The main features of the $g_{OO}(r)$ curves are reported in Table II. As can be seen, there is a good agreement between the two curves; the fact the oscillations of our computed curve are slightly reduced with respect to the experimental one can again be related to the higher effective temperature of our simulation.

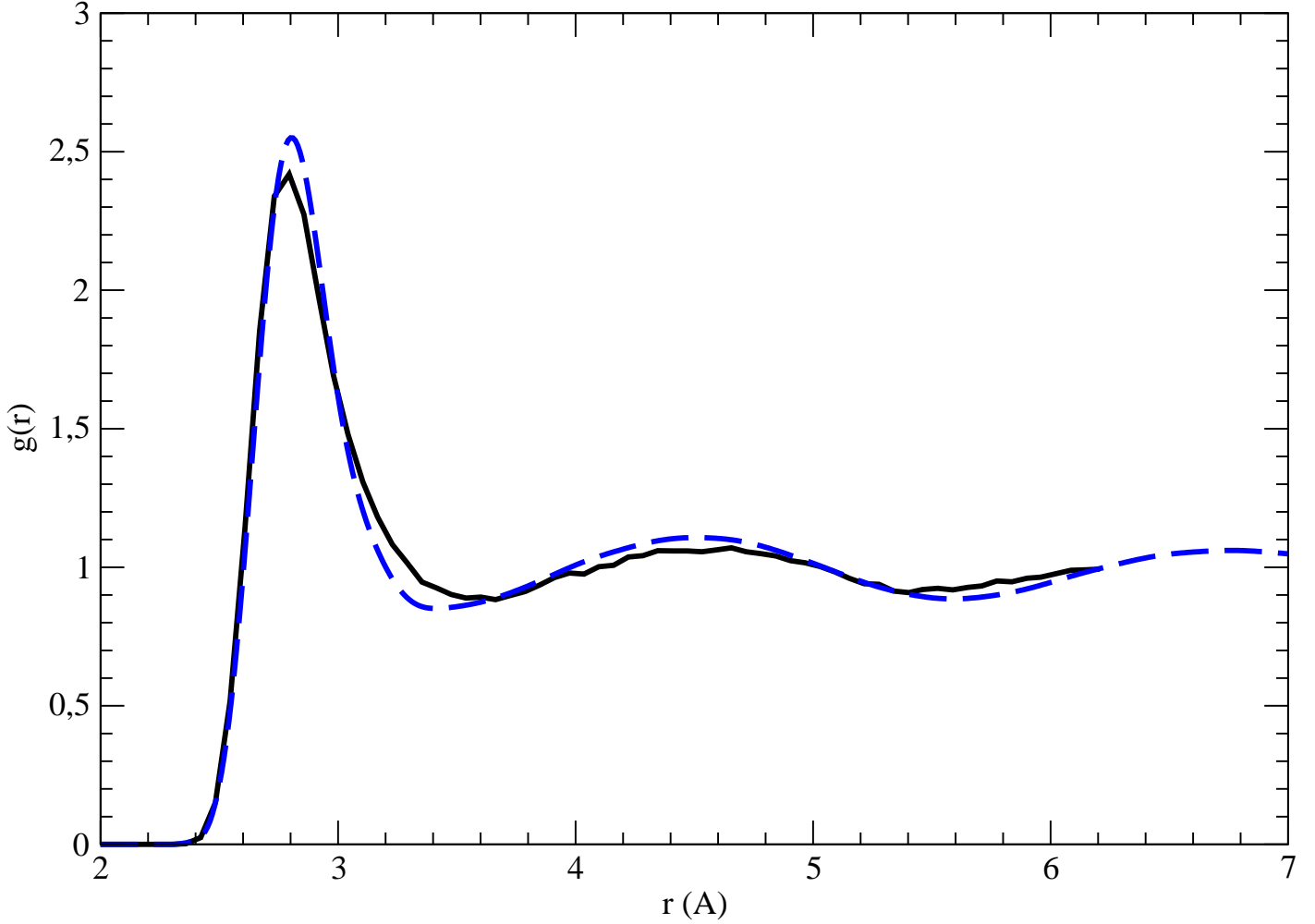


FIG. 13: O-O pair correlation function, $g_{OO}(r)$, compared with that obtained experimentally from X-ray diffraction measurements at ambient conditions.⁷⁷⁻⁷⁹

In Fig. 14, for liquid Ar our computed Ar-Ar pair correlation function, $g(r)$, is compared with that obtained experimentally from neutron-scattering measurements at 85 K,⁸² while again the main features of the $g(r)$ curves are reported in Table II. Even in this case there is a reasonable agreement between the simulation and experimental curve, by considering that simulations for liquid Ar have been performed at significantly higher temperature (129 K) than experiments (85 K) (note that the experimental melting and boiling points of Ar are at 84 and 87 K, respectively). After applying the same finite-size correction adopted

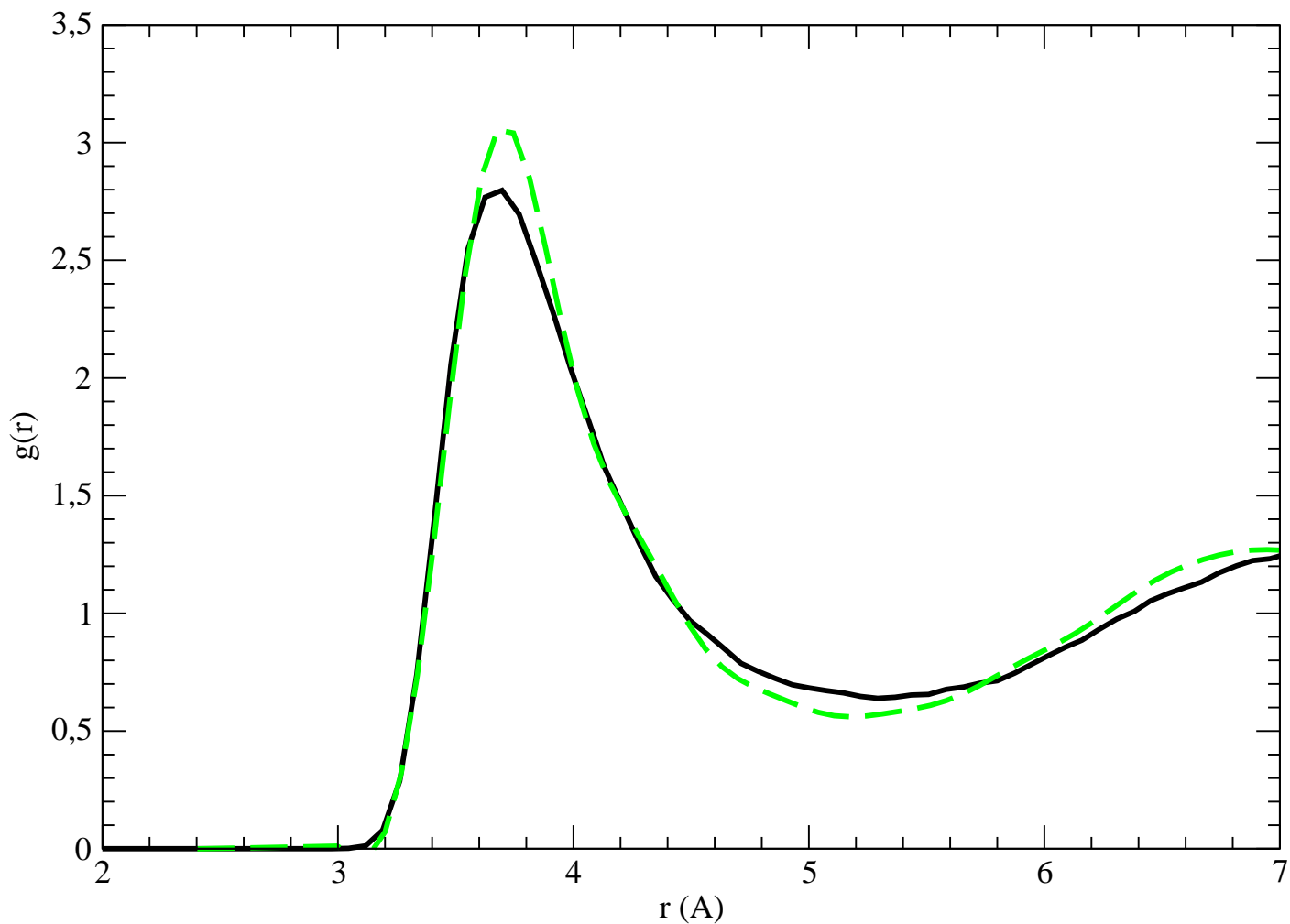


FIG. 14: Ar-Ar pair correlation function, $g(r)$, compared with that obtained experimentally from neutron-scattering measurements at 85K.⁸²

above for liquid water, our estimated diffusion coefficient for liquid Ar, $D = 3.82 \times 10^{-5}$ cm²/s, evaluated at a nominal simulation temperature of 129 K is significantly higher than the reference value (1.6×10^{-5} cm²/s) reported at 84 K.⁸⁰ Again this discrepancy can be explained in terms of the higher temperature of the liquid Ar simulation.

IV. CONCLUSIONS

Shear and bulk viscosity of liquid water and Argon have been evaluated, together with other structural and dynamical properties, from first principles by adopting a vdW-corrected DFT approach, by performing Molecular Dynamics simulations in the NVE ensemble and using the Kubo-Greenwood equilibrium approach. For liquid Argon the thermal conductivity has been also calculated. Concerning liquid water, to our knowledge this is the first estimate of the bulk viscosity and of the shear-viscosity/bulk-viscosity ratio from first principles. By analyzing our results and comparing them with reference experimental data, we can conclude that our first-principles simulations, performed at a nominal average temperature of 366 K to guarantee that the systems is liquid-like, actually describe well the basic dynamical properties of liquid water at about 330 K. In comparison with liquid water, the normal, monatomic liquid Ar is characterized by a much smaller bulk-viscosity/shear-viscosity ratio (close to unity) and this feature is well reproduced by our first-principles approach which predicts a value of the ratio in better agreement with experimental reference data than that obtained using the empirical Lennard-Jones potential. The computed thermal conductivity of liquid Argon is also in good agreement with the experimental value.

V. ACKNOWLEDGEMENTS

We acknowledge S. Baroni for useful discussions and funding from Fondazione Cariparo, Progetti di Eccellenza 2017, relative to the project: "Engineering van der Waals Interactions: Innovative paradigm for the control of Nanoscale Phenomena".

VI. DATA AVAILABILITY

The data that support the findings of this study are available from the corresponding author upon reasonable request.

¹ M. P. Allen and D. J. Tildesley, *Computer Simulations of Liquids* (Oxford Science Publications, Clarendon Press, Oxford 1987).

- ² E. Helfand, "Transport Coefficients from Dissipation in a Canonical Ensemble", *Phys. Rev.* **119**, 1 (1960).
- ³ B. J. Alder, D. M. Gass, T. E. Wainwright, "Studies in Molecular Dynamics. VIII. The Transport Coefficients for a Hard-Sphere Fluid", *J. Chem. Phys.* **53**, 3813 (1970).
- ⁴ E. M. Gosling, I. R. McDonald, K. Singer, "On the calculation by molecular dynamics of the shear viscosity of a simple fluid", *Mol. Phys.* **26**, 1475 (1973).
- ⁵ G. Ciccotti, G. Jacucci, I. R. McDonald, "Transport properties of molten alkali halides", *Phys. Rev. A* **13**, 426 (1976).
- ⁶ G. Ciccotti, G. Jacucci, K. R. McDonald, "Thermal response to a weak external field", *J. Phys. C: Solid State Phys.* **11**, L509 (1978).
- ⁷ G. Ciccotti, G. Jacucci, I. R. McDonald, "Thought-experiments by molecular dynamics", *J. Stat. Phys.* **21**, 1 (1979).
- ⁸ M. Schoen, C. Hoheisel, "The shear viscosity of a Lennard-Jones fluid calculated by equilibrium molecular dynamics", *Mol. Phys.* **56**, 653 (1985).
- ⁹ C. Hoheisel, "Bulk viscosity of model fluids. A comparison of equilibrium and nonequilibrium molecular dynamics results", *J. Chem. Phys.* **86**, 2328 (1987).
- ¹⁰ J. J. Erpenbeck, "Einstein-Kubo-Helfand and McQuarrie relations for transport coefficients", *Phys. Rev. E* **51**, 4296 (1995).
- ¹¹ S. Balasubramanian, C. J. Mundy, M. L. Klein, "Shear viscosity of polar fluids: Molecular dynamics calculations of water", *J. Chem. Phys.* **105**, 11190 (1996).
- ¹² D. Alfé, M. J. Gillan, "First-principles calculation of transport coefficients", *Phys. Rev. Lett.* **81**, 5161 (1998).
- ¹³ G.-J. Guo, Y. Zhang, "Equilibrium molecular dynamics calculation of the bulk viscosity of liquid water", *Mol. Phys.* **99**, 283 (2001).
- ¹⁴ S. Viscardy, J. Servantie and P. Gaspard, "Transport and Helfand moments in the Lennard-Jones fluid. I. Shear viscosity", *J. Chem. Phys.* **126**, 184512 (2007).
- ¹⁵ R. E. Jones, K. K. Mandadapu, "Adaptive Green-Kubo estimates of transport coefficients from molecular dynamics based on robust error analysis", *J. Chem. Phys.* **136**, 154102 (2012).
- ¹⁶ S. V. Lishchuk, "Role of three-body interactions in formation of bulk viscosity in liquid argon", preprint (2012): arXiv:1204.1235 [cond-mat.soft]
- ¹⁷ C. Kim, O. Borodin, G. Emkarniadakis, "Quantification of sampling uncertainty for molecular

- dynamics simulation: Time-dependent diffusion coefficient in simple fluids”, *J. Comput. Phys.* **302**, 485 (2015).
- ¹⁸ E. M. Kirova, G. E. Norman, ”Viscosity calculations at molecular dynamics simulations”, *Journal of Physics: Conference Series* **653**, 012106 (2015).
- ¹⁹ Y. Shi, H. Scheiber, R. Z. Khaliullin, ”Contribution of the Covalent Component of the Hydrogen-Bond Network to the Properties of Liquid Water”, *J. Phys. Chem. A* **122**, 7482 (2018).
- ²⁰ F. Z. Chen, N. A. Mauro, S. M. Bertrand, P. McGrath, L. Zimmer, K. F. Kelton, ”Breakdown of the Stokes-Einstein relationship and rapid structural ordering in CuZrAl metallic glass-forming liquids”, *J. Chem. Phys.* **155**, 104501 (2021).
- ²¹ R. Rabani, M. H. Saidi, L. Joly, S. Merabia, A. Rajabpour, ”Enhanced local viscosity around colloidal nanoparticles probed by equilibrium molecular dynamics simulations”, *J. Chem. Phys.* **155**, 174701 (2021).
- ²² H. Kusudo, T. Omori, Y. Yamaguchi, ”Local stress tensor calculation by the method-of-plane in microscopic systems with macroscopic flow: A formulation based on the velocity distribution function”, *J. Chem. Phys.* **155**, 184103 (2021).
- ²³ A. Torres, L. S. Pedroza, M. Fernandez-Serra, A. R. Rocha, ”Using Neural Network Force Fields to Ascertain the Quality of Ab Initio Simulations of Liquid Water”, *J. Phys. Chem. B* **125**, 10772 (2021).
- ²⁴ R. Vogelsang, C. Hoheisel, G. Ciccotti, ”Thermal conductivity of the Lennard-Jones liquid by molecular dynamics calculations”, *J. Chem. Phys.* **86**, 6371 (1987).
- ²⁵ Z. Fan, L. F. C. Pereira, H.-Q. Wang, J.-C. Zheng, D. Donadio, A. Harju, ”Force and heat current formulas for many-body potentials in molecular dynamics simulations with applications to thermal conductivity calculations”, *Phys. Rev. B* **92**, 094301 (2015).
- ²⁶ J. Kang, L.-W. Wang, ”First-principles Green-Kubo method for thermal conductivity calculations”, *Phys. Rev. B* **96**, 020302(R) (2017).
- ²⁷ M. French, ”Thermal conductivity of dissociating water—an ab initio study”, *New J. Phys.* **21**, 023007 (2019).
- ²⁸ G. A. Fernandez, J. Vrabec, and H. Hasse, ”A molecular simulation study of shear and bulk viscosity and thermal conductivity of simple real fluids”, *Fluid Phase Equilibria* **221**, 157 (2004).
- ²⁹ A. Marcolongo, P. Umari, S. Baroni, ”Microscopic theory and quantum simulation of atomic heat transport”, *Nat. Phys.* **12**, 80 (2016).

- ³⁰ L. Ercole, A. Marcolongo, P. Umari, S. Baroni, "Gauge Invariance of Thermal Transport Coefficients", *J. Low. Temp. Phys.* **185**, 79 (2016).
- ³¹ A. Marcolongo, R. Bertossa, D. Tisi, S. Baroni, "QEHeat: An open-source energy flux calculator for the computation of heat-transport coefficients from first principles", *Comput. Phys. Commun.* **269**, 108090 (2021).
- ³² D. Tisi, L. Zhang, R. Bertossa, H. Wang, R. Car, S. Baroni, "Heat transport in liquid water from first-principles and deep neural network simulations", *Phys. Rev. B* **104**, 224202 (2021).
- ³³ C. Malosso, L. Zhang, R. Car, S. Baroni, D. Tisi, "Viscosity in water from first-principles and deep-neural-network simulations", *Npj Comput. Mater.* **8**, 139 (2022).
- ³⁴ L. Ercole, A. Marcolongo, S. Baroni, "Accurate thermal conductivities from optimally short molecular dynamics simulations", *Sci. Rep.* **7**, 15835 (2017).
- ³⁵ L. Ercole, R. Bertossa, S. Bisacchi, S. Baroni, "SporTran: A code to estimate transport coefficients from the cepstral analysis of (multivariate) current time series", *Comput. Phys. Commun.* **280**, 108470 (2022).
- ³⁶ M. S. Green, "Markoff Random Processes and the Statistical Mechanics of Time-Dependent Phenomena. II. Irreversible Processes in Fluids", *J. Chem. Phys.* **22**, 398 (1954).
- ³⁷ R. Kubo, M. Yokota, and S. Nakajima, "Statistical-Mechanical Theory of Irreversible Processes. II. Response to Thermal Disturbance", *J. Phys. Soc. Jpn* **12**, 1203 (1957).
- ³⁸ D. McQuarrie, "Electronic Transport in Mesoscopic Systems", (University Science Books, Sausalito, 2000).
- ³⁹ R. Hafner, G. Guevara-Carrion, J. Vrabec, P. Klein, "Sampling the Bulk Viscosity of Water with Molecular Dynamics Simulation in the Canonical Ensemble", *J. Phys. Chem. B* **126**, 10172 (2022).
- ⁴⁰ A. Yahya, L. Tan, S. Perticaroli, E. Mamontov, D. Pajerowski, J. Neufeind, G. Ehlersd, J. D. Nickels, "Molecular origins of bulk viscosity in liquid water", *Phys. Chem. Chem. Phys.* **22**, 9494 (2020).
- ⁴¹ A. S. Dukhin and P. J. Goetz, "Bulk viscosity and compressibility measurement using acoustic spectroscopy", *J. Chem. Phys.* **130**, 124519 (2009).
- ⁴² R. Car and M. Parrinello, "Unified Approach for MD and DFT", *Phys. Rev. Lett.* **55**, 2471 (1985). We have used the code CPMD: <http://www.cpmc.org/>, Copyright IBM Corp 1990-2022, Copyright MPI für Festkörperforschung Stuttgart 1997-2001.

- ⁴³ N. Troullier and J. L. Martins, "Efficient pseudopotentials for plane-wave calculations", *Phys. Rev. B* **43**, 1993 (1991).
- ⁴⁴ A. D. Becke, "Density-functional exchange energy approximation with correct asymptotic behavior", *Phys. Rev. A* **38**, 3098 (1988); C. Lee, W. Yang, and R. C. Parr, "Development of the Colle-Salvetti correlation energy formula into a functional of the electron density", *Phys. Rev. B* **37**, 785 (1988).
- ⁴⁵ S. Grimme, "Semiempirical GGA-type density functional constructed with a long-range dispersion correction", *J. Comp. Chem.* **27**, 1787 (2006).
- ⁴⁶ M. Sprik, J. Hutter, and M. Parrinello, "Ab initio MD simulation of liquid water: Comparison of 3 gradient-corrected density functionals", *J. Chem. Phys.* **105**, 1142 (1996).
- ⁴⁷ P. L. Silvestrelli and M. Parrinello, "Water Molecule Dipole in the Gas and in the Liquid Phase", *Phys. Rev. Lett.* **82**, 3308 (1999).
- ⁴⁸ P. L. Silvestrelli and M. Parrinello, "Structural, electronic, and bonding properties of liquid water from first principles", *J. Chem. Phys.* **111**, 3572 (1999).
- ⁴⁹ M. Boero, K. Terakura, T. Ikeshoji, C. C. Liew, and M. Parrinello, "Hydrogen Bonding and Dipole Moment of Water at Supercritical Conditions: A First-Principles Molecular Dynamics Study", *Phys. Rev. Lett.* **85**, 3245 (2000).
- ⁵⁰ M. Boero, K. Terakura, T. Ikeshoji, C. C. Liew, and M. Parrinello, "Water at Supercritical Conditions: A First-Principles Study", *J. Chem. Phys.* **115**, 2219 (2001).
- ⁵¹ P. L. Silvestrelli, "Van der Waals Interactions in DFT Made Easy by Wannier Functions", *Phys. Rev. Lett.* **100**, 053002 (2008).
- ⁵² P. L. Silvestrelli, K. Benyahia, S. Grubisic, F. Ancilotto, and F. Toigo, "Van der Waals interactions at surfaces by density functional theory using Wannier functions", *J. Chem. Phys.* **130**, 074702 (2009).
- ⁵³ P. L. Silvestrelli, "Van der Waals Interactions in DFT using Wannier Functions", *J. Phys. Chem. A* **113**, 5224 (2009).
- ⁵⁴ F. O. Kannemann and A. D. Becke, "Van der Waals Interactions in Density-Functional Theory: Rare-Gas Diatomics", *J. Chem. Theory Comput.* **5**, 719 (2009).
- ⁵⁵ J. Schmidt, J. VandeVondele, I.-F. W. Kuo, D. Sebastiani, J. I. Siepmann, J. Hutter, C. J. Mundy, "Isobaric-Isothermal Molecular Dynamics Simulations Utilizing Density Functional Theory: An Assessment of the Structure and Density of Water at Near-Ambient Conditions",

- J. Phys. Chem. B **113**, 11959 (2009).
- ⁵⁶ J. Wang, G. Román-Pérez, J. M. Soler, E. Artacho, M.-V. Fernández-Serra, "Density, structure, and dynamics of water: The effect of van der Waals interactions", J. Chem. Phys. **134**, 024516 (2011).
- ⁵⁷ S. Yoo and S. S. Xantheas, "Communication: The effect of dispersion corrections on the melting temperature of liquid water", J. Chem. Phys. **134**, 121105 (2011).
- ⁵⁸ J. C. Grossman, E. Schwegler, E. W. Draeger, F. Gygi, G. Galli, "Towards an assessment of the accuracy of density functional theory for first principles simulations of water", J. Chem. Phys. **120**, 300 (2004).
- ⁵⁹ J. P. Perdew, K. Burke, and M. Ernzerhof, "Generalized Gradient approximation made simple", Phys. Rev. Lett. **77**, 3865 (1996).
- ⁶⁰ D. Frenkel and R. Smit, Understanding Molecular Simulation (Academic Press, San Diego, 1996).
- ⁶¹ C. Herrero, M. Pauletti, G. Tocci, M. Iannuzzi, L. Joly, "Connection between water's dynamical and structural properties: Insights from ab initio simulations", PNAS **119**, e2121641119 (2022).
- ⁶² T. A. Litovitz, E. H. Carnevale, "Effect of Pressure on Sound Propagation in Water", J. Appl. Phys. **26**, 816 (1955).
- ⁶³ J. V. Sengers, J. T. R. Watson, "Improved International Formulations for the Viscosity and Thermal Conductivity of Water Substance", J. Phys. Chem. Ref. Data **15**, 1291 (1986).
- ⁶⁴ K. R. Harris and L. A. Woolf, "Temperature and Volume Dependence of the Viscosity of Water and Heavy Water at Low Temperatures", J. Chem. Eng. Data **49**, 1064 (2004).
- ⁶⁵ M. J. Holmes, N. G. Parker, M. J. W. Povey, "Temperature dependence of bulk viscosity in water using acoustic spectroscopy", J. Phys.: Conf. Ser. **269**, 012011 (2011).
- ⁶⁶ J. A. Cowan, R. N. Ball, "Temperature dependence of bulk viscosity in liquid argon", Can. J. Phys. **50**, 1881 (1972).
- ⁶⁷ P. J. Linstrom, G. W. Mallard eds., NIST Chemistry WebBook, NIST Standard Reference Database Number 69
- ⁶⁸ J. Sun, A. Ruzsinszky, J. P. Perdew, "Strongly constrained and appropriately normed semilocal density functional", Phys. Rev. Lett. **115**, 036402 (2015).
- ⁶⁹ J. Klimeš, D. R. Bowler, A. Michaelides, "Chemical accuracy for the van der Waals density functional", J. Phys. Condens.Matter **22**, 022201 (2010); "Van der Waals density functionals

- applied to solids”, *Phys. Rev. B* **83**, 195131 (2011).
- ⁷⁰ B. A. Younglove and H. J. M. Hanley, ”The Viscosity and Thermal Conductivity Coefficients of Gaseous and Liquid Argon”, *Journal of Physical and Chemical Reference Data* **15**, 1323 (1986).
- ⁷¹ C. Hoheisel, R. Vogelsang and M. Schoen, ”Bulk viscosity of the Lennard-Jones fluid for a wide range of states computed by equilibrium molecular dynamics”, *J. Chem. Phys.* **87**, 7195 (1987).
- ⁷² C. M. Davis, J. Jarzynski, “Water: A Comprehensive Treatise, Vol. 1, edited by F. Franks (1972) p. 443.
- ⁷³ O. Reynolds, ”IV. On the theory of lubrication and its application to Mr. Beauchamp tower’s experiments, including an experimental determination of the viscosity of olive oil”, *Phil. Trans. R. Soc. Lond.* **177**, 157 (1886).
- ⁷⁴ See, for instance, values tabulated in <https://dtrx.de/od/diff/>
- ⁷⁵ T. A. Litovitz and C. M. Davis, ”Physical Acoustics”, Vol. 2, edited by W. P. Mason, New York: Academic, Chap. 5.
- ⁷⁶ J. Xu, X. Ren, W. Gong, R. Dai, D. Liu, ”Measurement of the bulk viscosity of liquid by Brillouin scattering”, *Appl. Opt.* **42**, 6704 (2003).
- ⁷⁷ L. B. Skinner, C. Huang, D. Schlesinger, L. G. M. Pettersson, A. Nilsson, C. J. Benmore, ”Benchmark oxygen-oxygen pair-distribution function of ambient water from x-ray diffraction measurements with a wide Q-range”, *J. Chem. Phys.* **138**, 074506 (2013).
- ⁷⁸ L. B. Skinner, C. J. Benmore, J. C. Neufeind, J. B. Parise, ”The structure of water around the compressibility minimum”, *J. Chem. Phys.* **141**, 214507 (2014).
- ⁷⁹ J. Daru, H. Forbert, J. Behler, D. Marx, ”Coupled Cluster Molecular Dynamics of Condensed Phase Systems Enabled by Machine Learning Potentials: Liquid Water Benchmark”, *Phys. Rev. Lett.* **129**, 226001 (2022).
- ⁸⁰ J.-P. Hansen, I. R. McDonald, ”Theory of simple liquids”, Academic Press (1990).
- ⁸¹ E. H. Hardy, A. Zygar, M. D. Zeidler, M. Holz, F. D. Sacher, ”Isotope effect on the translational and rotational motion in liquid water and ammonia”, *J. Chem. Phys.* **114**, 3174 (2001).
- ⁸² J. L. Yarnell, M. J. Katz, and R. G. Wenzel, ”Structure Factor and Radial Distribution Function for Liquid Argon at 85 K”, *Phys. Rev. A* **7**, 2130 (1973).